

Structural and Magnetic Properties in $\text{Nd}_{0.7}\text{Sr}_{0.3}\text{MnO}_3$ Manganite

Feng Xiaomei^{*}, Chen Jiankun, Shen Yifu, Unisha Shilpakar,
Wang Ding, Huang Guoqiang

College of Material Science and Technology, Nanjing University of Aeronautics and
Astronautics, Nanjing 210016, P. R. China

(Received 22 August 2015; revised 16 November 2015; accepted 5 January 2016)

Abstract: The temperature evolution of the crystal structure for $\text{Nd}_{0.5}\text{Sr}_{0.5}\text{MnO}_3$ has been investigated by powder XRD between 125 K and 725 K. The structure can be described with a monoclinic symmetry (space group $P2_1/m$) in the temperature range of 125–175 K, while with the increase in temperature between 175 K and 575 K the structure involves a higher orthorhombic symmetry (space group Imma). The rhombohedral structure with space group $R\bar{3}c$ is observed at high temperature region of 575–725 K. The increase in the magnetization at low temperatures can be ascribed to the field-induced short-range magnetic order of the Nd^{3+} ions. The dc and ac susceptibility data show some anomalies around the FM-PM transition region which can be attributed to the glass behavior and magnetic relaxation.

Key words: manganite; powder X-ray diffraction; crystal structure; magnetic susceptibility; perovskite

CLC number: O469 **Document code:** A **Article ID:** 1005-1120(2017)04-0393-05

0 Introduction

In the previous work of charge-ordered compound $\text{Nd}_{0.5}\text{Sr}_{0.5}\text{MnO}_3$, it has been shown that phase transition is a function of temperature. $\text{Nd}_{0.5}\text{Sr}_{0.5}\text{MnO}_3$ undergoes a transition from a paramagnetic (PM) insulator at room temperature to a ferromagnetic (FM) metal below 250 K, and finally to an A-type antiferromagnetic (AFM) state below 225 K followed by the transition to a charge-ordered CE-type AFM phase at a lower temperature of 150 K. The ground state consists of not only FM and CE-type AFM phase but also A-type AFM phase^[1-6].

$\text{Nd}_{0.5}\text{Sr}_{0.5}\text{MnO}_3$ has an orthorhombic perovskite-type structure, some authors determined the symmetry as Pnma ^[7] or Pbnm ^[5, 8], while some others reported the symmetry as Imma that will be changed to monoclinic $P2_1/m$ symmetry below 150 K^[3, 4, 9]. The low temperature monoclinic structure coincides with the appearance of CE-type AFM phase.

Here, we present our studies of the temperature dependent X-ray diffraction (XRD) measure-

ments on $\text{Nd}_{0.5}\text{Sr}_{0.5}\text{MnO}_3$ in a large temperature range. We also demonstrate the magnetic characteristics of this half-doped manganite.

1 Experiments

Polycrystalline samples of $\text{Nd}_{0.5}\text{Sr}_{0.5}\text{MnO}_3$ were prepared from stoichiometric amounts of Nd_2O_3 (99.9%), SrCO_3 (99%) and MnO_2 (97.5%). As most of the rare earth oxides absorb moisture from the air, Nd_2O_3 has been preheated at 1 000 °C for 12 h. All the powders were mixed and grinded for a long time in order to produce a homogeneous mixture. First, the mixture was heated at 900 °C for 24 h and calcined at 1 200 °C for 24 h with intermediate grindings. After that, the reaction product was then finely pulverized and cold pressed into 10 mm diameter discs under 30 MPa, sintered in air at 1 400 °C for one day, then slowly cooled to the room temperature.

Powder XRD data below room temperature were carried out with a Rigaku D/max 2 500 diffractometer while powder X-ray diffraction (XRD) data at high temperature region were col-

^{*} Corresponding author, E-mail address: fengxm@nuaa.edu.cn.

lected on a PANalytical X'pert PRO Alpha-1 diffractometer (CuK radiation, $\lambda = 1.5406 \text{ \AA}$) at 45 kV and 40 mA. A step scan mode was employed with a step width of $2\theta = 0.017^\circ$ and a count time of 2 s per step. The Rietveld refinements were performed using the profile fitting program FULLPROF^[10]. The magnetization measurements were performed with a MPMS-7 SQUID magnetometer from quantum design.

2 Results and Discussions

2.1 Structure

The room temperature powder XRD patterns of $\text{Nd}_{0.5}\text{Sr}_{0.5}\text{MnO}_3$ give satisfying result fitting to an orthorhombic structure with *Imma* symmetry. Our refined lattice parameters are $a = 5.471478(45) \text{ \AA}$, $b = 7.634183(63) \text{ \AA}$, $c = 5.429764(49) \text{ \AA}$. The refinement converged to give an agreement factor $R_{\text{wp}} = 23\%$, $R_{\text{exp}} = 21.31\%$ and $\chi^2 = 1.17$. Observed, calculated, and difference diffraction profiles are shown in Fig. 1. The stars and solid continuous lines represent observed and calculated pattern respectively. The difference plot is shown at the bottom of Fig. 1. Positions for the Bragg reflections are marked by vertical bars. The lattice parameters agree well with the previously reported results^[3, 4, 9].

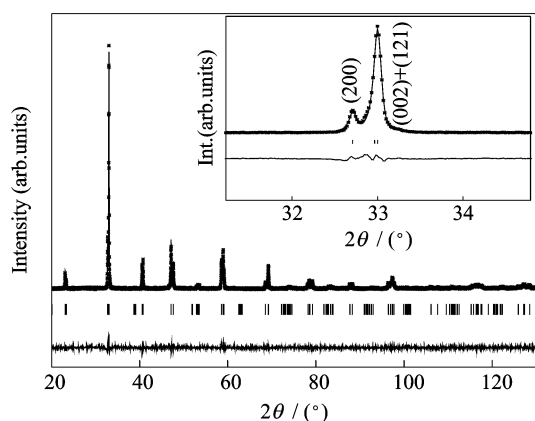


Fig. 1 Rietveld refinement profile of powder XRD pattern for $\text{Nd}_{0.5}\text{Sr}_{0.5}\text{MnO}_3$ at 300 K with *Imma* structural model

On cooling the samples, changes of the XRD patterns were observed as illustrated in Fig. 2, especially the reflection at about 47° in 2θ is gradually split into two sharp and distinct peaks from 300 K to 125 K. The powder XRD patterns be-

tween 275 K and 200 K could also be indexed with an orthorhombic *Imma* lattice, while the XRD patterns below 200 K give good fits to a monoclinic *P21/m* lattice. Our low temperature XRD results confirm the change of symmetry accompanying the magnetic phase transitions as reported in several previous studies^[3-5, 7-9].

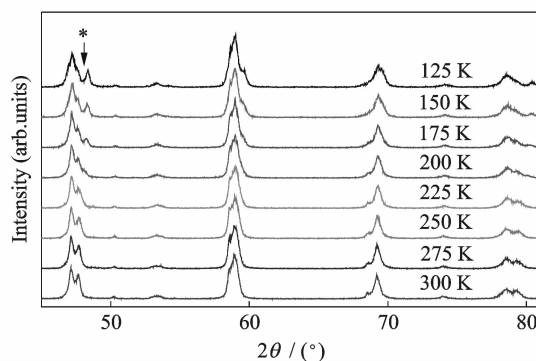


Fig. 2 Low temperature XRD patterns of $\text{Nd}_{0.5}\text{Sr}_{0.5}\text{MnO}_3$

The powder XRD patterns of $\text{Nd}_{0.5}\text{Sr}_{0.5}\text{MnO}_3$ over the temperature range of 300–725 K (Fig. 3) indicate that around 575 K there was a change of crystal symmetry. Below 575 K, all of the observed peaks satisfied the reflection conditions of hkl : $h+k+l=2n$; and $hk0$: $h=2n$, being consistent with the *Imma* symmetry as reported by Caignaert et al^[9]. At and above 575 K, the peaks in each pattern can be indexed on the basis of a rhombohedral unit cell (space group *R-3c*). The cell symmetry was identified by the observation of the reflection based on the limiting condition on hkl : $-h+k+l=3n$ ^[11]. Fig. 4 shows the XRD refinement for $\text{Nd}_{0.5}\text{Sr}_{0.5}\text{MnO}_3$ at 725 K, where stars are the experimental data, line is the Rietveld fit, and the lower line is the difference curve. Positions for the Bragg reflections are marked by vertical bars. Calculation was carried out supposing space group *R-3c*. This whole pattern fitting led to an agreement factor $R_{\text{wp}} = 19.7\%$, $R_{\text{exp}} = 18.15\%$ and $\chi^2 = 1.18$. The inset shows the result of the Rietveld refinement of the first strong peak. This type of splitting of the main peak indicates the rhombohedral distortion of lattice^[12]. The temperature evolution of the unit cell parameters is shown in Fig. 5, where squares, circles, and triangles represent the a , $b/\sqrt{2}$, and c lattice parameters, respectively. The orthorhombic phase is represented by open sym-

bols, while the data points for the rhombohedral phase are filled. Lines are shown only as guides to the eye.

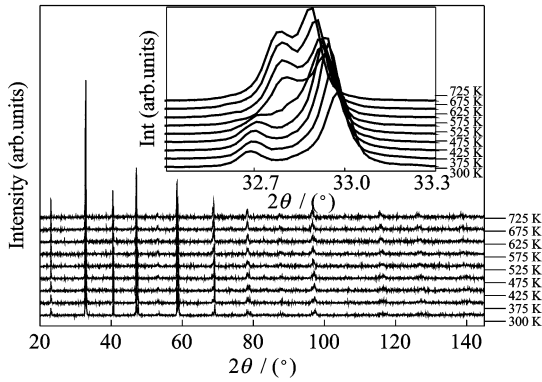


Fig. 3 High temperature XRD patterns of $\text{Nd}_{0.5}\text{Sr}_{0.5}\text{MnO}_3$

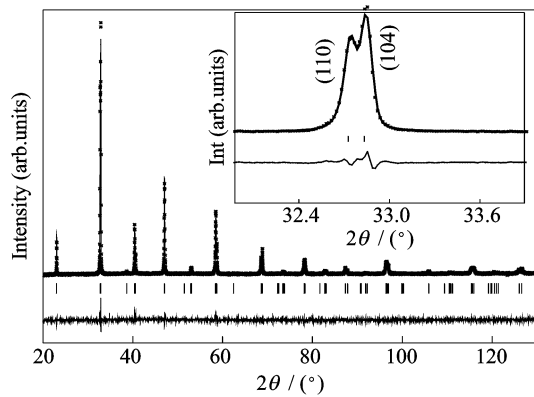


Fig. 4 Rietveld refinement plot of the powder XRD data at 725 K

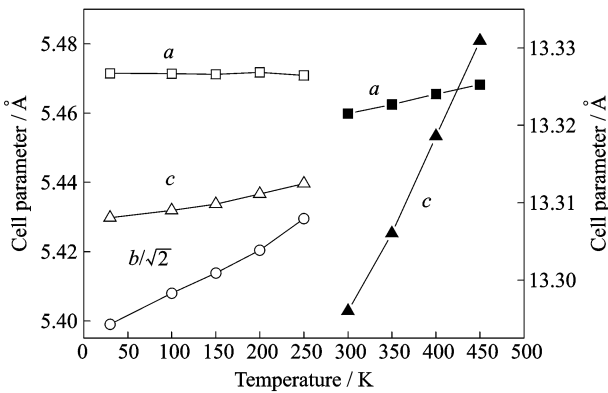


Fig. 5 Lattice parameters of $\text{Nd}_{0.5}\text{Sr}_{0.5}\text{MnO}_3$ as a function of temperature

2.2 Magnetization measurements

Fig. 6 shows the zero field-cooled (ZFC) temperature dependent magnetization data recorded at different applied fields during warming the samples up to 300 K. As shown in the inset of Fig. 6, $\text{Nd}_{0.5}\text{Sr}_{0.5}\text{MnO}_3$ firstly undergoes PM-FM phase transition at around 275 K (T_C) and FM-

AFM transition at around 160 K. The transition temperatures are in agreement with those reported in literature for bulk samples^[1-5]. To further examine the influence of the applied magnetic field on the system, magnetization measurements with different applied magnetic field up to 5 T were studied. We found that the higher the applied magnetic field, the higher magnetization is in both AFM and FM states. Furthermore, the magnetization at low temperatures ($5 \text{ K} \leq T \leq 50 \text{ K}$) showed a rapid increase with decreasing temperatures when the applied fields exceed 1 T. Gordon et al.^[13] and Nam et al.^[14] attributed this anomaly to the Nd-Nd exchange interactions. Millange's neutron data at 1.7 K supported this suggestion, they found that there were ferromagnetic scattering arising from both manganese and neodymium along the b axis^[15]. However, López et al. attributed it to a possible short-range ordering of the Nd^{3+} ions because the Nd^{3+} ions did not show a long range magnetic order until the lowest measured temperatures in the neutron diffraction studies^[16-18]. Our results confirm that the increase in the magnetization at low temperatures is produced by the field-induced short-range magnetic order of the Nd^{3+} ions.

In order to obtain further insight into the magnetic properties of the samples, the dc and ac magnetic susceptibilities measurements have been carried out.

After cooling down from room temperature without applied field (ZFC), susceptibility χ was

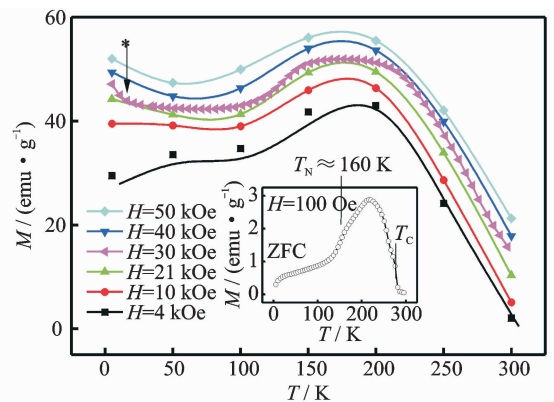


Fig. 6 Temperature dependence of magnetization using different applied magnetic field in ZFC conditions. The inset shows the $M_{\text{ZFC}}(T)$ data of $\text{Nd}_{0.5}\text{Sr}_{0.5}\text{MnO}_3$ taken on warming in an applied field of $H_{\text{ex}} = 100 \text{ Oe}$

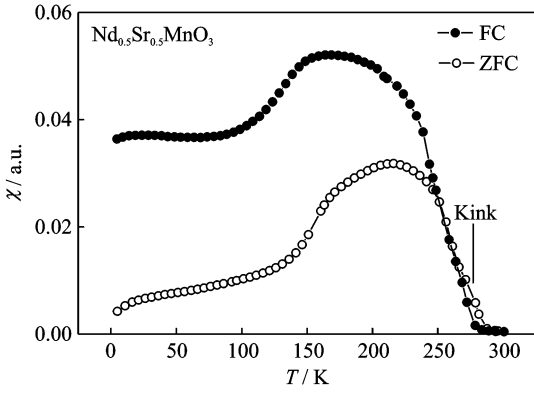
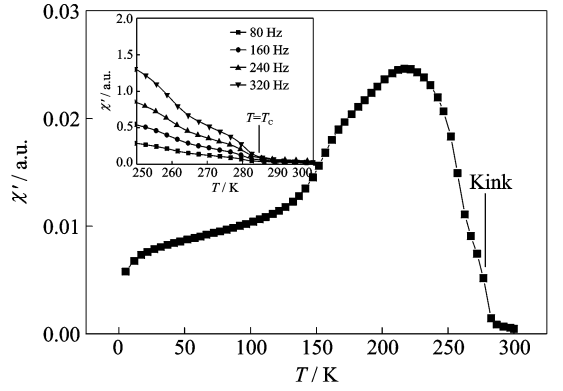


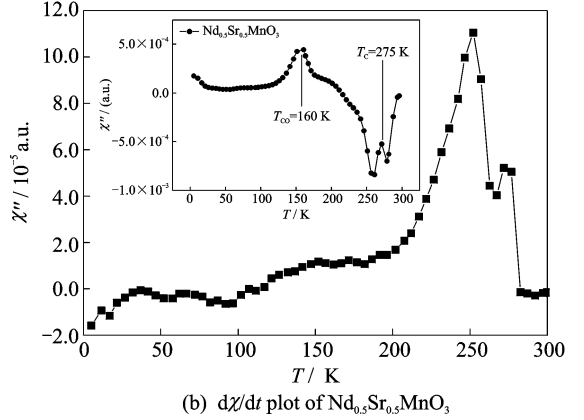
Fig. 7 dc susceptibility χT curves for $\text{Nd}_{0.5}\text{Sr}_{0.5}\text{MnO}_3$ in ZFC and FC conditions

subsequently measured heating from 5 K to 300 K and cooling from 300 K to 5 K under an applied field 100 Oe (FC) (shown in Fig. 7). In such a temperature cycle, a pronounced difference between curves is observed. The large splitting of the FC and ZFC magnetization curves is a signature of the conventional spin glass. Furthermore, in the temperature region close to T_C , there appears a kink in the ZFC curve (the arrow indication) which leads to the irreversibility between the FC and ZFC magnetization. AC susceptibility measurements were used to search for the magnetic glassy behavior and the hysteresis of $\chi(T)$ at FM-PM transition region.

In Fig. 8, we present the temperature dependence of the in-phase $\chi'(T)$ and the corresponding out-of-phase $\chi''(T)$. The real and imaginary parts of the ac susceptibility were measured in an 1 Oe ac field and 332 Hz frequency. The $\chi'(T)$ curve is quite similar to the dc $\chi-T$ (ZFC) plotted in Fig. 7. Also, kink at χ'_{ac} is observed at noted temperature interval. The inset of Fig. 8 (a) shows the $\chi'(T)$ curves measured at different frequencies. We observe a clear frequency dependence of the real components of ac susceptibility, which implies the presence of magnetic disorder and a spin-glass state in $\text{Nd}_{0.5}\text{Sr}_{0.5}\text{MnO}_3$. Moreover, it is notable that two χ'_{ac} peaks are observed around the FM-PM transition region. Meanwhile, we also find that the $d\chi/dt$ plot appears two local minimums nearby T_C (inset of Fig. 8(b)). This behavior in susceptibility can be interpreted to originate from the short time magnetic relaxation during the FM-PM transition^[14, 17, 19-21].



(a) $\chi'(T)$ curves of $\text{Nd}_{0.5}\text{Sr}_{0.5}\text{MnO}_3$ measured at different frequencies



(b) $d\chi/dt$ plot of $\text{Nd}_{0.5}\text{Sr}_{0.5}\text{MnO}_3$

Fig. 8 Temperature dependence of real and imaginary components of ac susceptibility for $\text{Nd}_{0.5}\text{Sr}_{0.5}\text{MnO}_3$ sample

3 Conclusions

A systematic investigation of crystal structure of $\text{Nd}_{0.5}\text{Sr}_{0.5}\text{MnO}_3$ have been conducted via the temperature dependent XRD measures. A transition from monoclinic crystal structure to orthorhombic and then to rhombohedral symmetry occurs as the temperature increases. The most important feature of this study concerns the appearance of R-3c rhombohedral structure at high temperature. Magnetic properties of $\text{Nd}_{0.5}\text{Sr}_{0.5}\text{MnO}_3$ have been represented. The increase in the magnetization at low temperatures is originated from the field-induced short-range magnetic order of the Nd^{3+} ions. The glass behavior and relaxation effect are signaled by a frequency dependent in $\chi'_{ac}(T)$ and two peaks in χ''_{ac} around the FM-PM transition region.

Acknowledgments

This work was supported by the Jiangsu Provincial Natural Science Foundation (No. BK20141411). The au-

thors thank Dr. Liu GY for the X-ray diffraction measurements and phase analysis.

References:

- [1] KUWAHARA H, TOMIOKA Y, ASAMITSU A, et al. A first-order phase transition induced by a magnetic field [J]. *Science*, 1995, 270: 961-963.
- [2] KAWANO H, KAJIMOTO R, YOSHIKAWA H, et al. Magnetic ordering and relation to the metal-insulator transition in $\text{Pr}_{1-x}\text{Sr}_x\text{MnO}_3$ and $\text{Nd}_{1-x}\text{Sr}_x\text{MnO}_3$ with $x=1/2$ [J]. *Phys Rev Lett*, 1997, 78 (22): 4253-4256.
- [3] WOODWARD P, COX D, VOGT T, et al. Effect of compositional fluctuations on the phase transition in $(\text{Nd}_{1/2}\text{Sr}_{1/2})\text{MnO}_3$ [J]. *Chem Mater*, 1999, 11 (12): 3528-3538.
- [4] RITTER C, MAHENDIRAN R, IBARRA M, et al. Direct evidence of phase segregation and magnetic-field-induced structural transition in $\text{Nd}_{0.5}\text{Sr}_{0.5}\text{MnO}_3$ by neutron diffraction [J]. *Phys Rev B*, 2000, 61: R9229-R9232.
- [5] KAJIMOTO R, YOSHIKAWA H, KAWANO H, et al. Hole-concentration-induced transformation of the magnetic and orbital structures in $\text{Nd}_{1-x}\text{Sr}_x\text{MnO}_3$ [J]. *Phys Rev B*, 1999, 60: 9506-9517.
- [6] AWAJIA S, WATANABE Y, MASAKIB T, et al. High field and low temperature X-ray study on phase segregation for $\text{Nd}_{0.5}\text{Sr}_{0.5}\text{MnO}_3$ powder and single crystal [J]. *Physica B*, 2003, 329-333: 824-825.
- [7] MORITOMO Y, KUWAHARA H, TOMIOKA Y, et al. Pressure effects on charge-ordering transitions in Perovskite manganites [J]. *Phys Rev B*, 1997, 55: 7549-7556.
- [8] ZHENG R K, HUANG R X, TANG A N, et al. Ultrasonic study of the $\text{Nd}_{0.5}\text{Sr}_{0.5}\text{MnO}_3$ manganite [J]. *J. Alloys Comp*, 2002, 345: 68-71.
- [9] CAIGNAERT V, MILLANGE F, HERVIEU M, et al. The manganite $\text{Nd}_{0.5}\text{Sr}_{0.5}\text{MnO}_3$: A rare distortion of the perovskite [J]. *Solid State Commun*, 1996, 99: 173-177.
- [10] RODRIGUEZ-CARVAJAL J. Recent advances in magnetic structure determination by neutron powder diffraction [J]. *Physica B*, 1993, 192: 55-69.
- [11] SHEN C, CHEN C, LIU R, et al. Internal chemical pressure effect and magnetic properties of $\text{La}_{0.6}(\text{Sr}_{0.4-x}\text{Ba}_x)\text{MnO}_3$ [J]. *J Solid State Chem*, 2001, 156: 117-121.
- [12] SHIMURA T, HAYASHI T, INAGUMA Y, et al. Magnetic and electrical properties of $\text{La}_y\text{A}_x\text{Mn}_w\text{O}_3$ ($A=\text{Na, K, Rb, and Sr}$) with perovskite-type structure [J]. *J Solid State Chem*, 1996, 124: 250-263.
- [13] GORDON J, FISHER R, JIA Y, et al. Specific heat of $\text{Nd}_{0.67}\text{Sr}_{0.33}\text{MnO}_3$ [J]. *Phys Rev B*, 1999, 59: 127-130.
- [14] NAM D N H, MATHIEU R, NORDBLAD P, et al. Ferromagnetism and frustration in $\text{Nd}_{0.7}\text{Sr}_{0.3}\text{MnO}_3$ [J]. *Phys Rev B*, 2000, 62: 1027-1032.
- [15] MILLANGE F, CAIGNAERT V, MATHER G, et al. Low temperature orthorhombic to monoclinic transition due to size effect in $\text{Nd}_{0.7}\text{Ca}_{0.3-x}\text{Sr}_x\text{MnO}_3$: Evidence for a new type of charge ordering [J]. *J Solid State Chem*, 1996, 127: 131-135.
- [16] LÓPEZA J, LISBOA-FILHO P, LIMAB O, et al. Study of magnetic and specific heat measurements at low temperatures in $\text{Nd}_{0.5}\text{Sr}_{0.5}\text{MnO}_3$, $\text{Nd}_{0.5}\text{Ca}_{0.5}\text{MnO}_3$ [J]. *J Magn Magn Mater*, 2002, 242/243/244/245: 683-685.
- [17] LÓPEZ J, LISBOA-FILHO P N, PASSOS W A C, et al. Magnetic relaxation behavior in $\text{La}_{0.5}\text{Ca}_{0.5}\text{MnO}_3$ and $\text{Nd}_{0.5}\text{Sr}_{0.5}\text{MnO}_3$ [J]. *Phys Rev B*, 2000, 63: 224422.
- [18] MILLANGE F, DE BRION S, CHOUTEAU G. Charge, orbital, and magnetic order in $\text{Nd}_{0.5}\text{Ca}_{0.5}\text{MnO}_3$ [J]. *Phys Rev B*, 2000, 62: 5619-5626.
- [19] KUNDU S, DAS A, NATH T, et al. Size-induced ferromagnetism and metallicity in $\text{Nd}_{0.5}\text{Sr}_{0.5}\text{MnO}_3$ nanoparticles: A neutron diffraction study [J]. *J Magn Magn Mater*, 2012, 324: 823-829.
- [20] NAM D, JONASON K, NORDBLAD P, et al. Coexistence of ferromagnetic and glassy behavior in the $\text{La}_{0.5}\text{Sr}_{0.5}\text{CoO}_3$ perovskite compound [J]. *Phys Rev B*, 1999, 59: 4189-4194.
- [21] ULYANOV A, QUANG H, LEE K, et al. Magnetic relaxation behavior in $\text{Nd}_{0.5}\text{Sr}_{0.5}\text{MnO}_3$: Observation of negative imaginary component of ac magnetic susceptibility [J]. *IEEE Transactions on Magnetics*, 2008, 44(11): 3060-3062.

Dr. **Feng Xiaomei** presently is an associated professor and a master student supervisor of the College of Material Science and Technology, Nanjing University of Aeronautics and Astronautics (NUAA). Her research interests focus on magnetic functional material and the relationship between structure and properties of magnetic functional material.

Mr. **Chen Jiankun** received a master's degree from the College of Material Science and Technology, NUAA in 2016. His research interests include magnetic functional material.

Prof. **Shen Yifu** presently is a professor and a doctoral student supervisor of the College of Material Science and Technology, NUAA. Research interests focus on friction stir welding/processing and mechanical alloying.

Mr. **Unisha Shilpakar** received a master's degree from the College of Material Science and Technology, NUAA in 2016. Research interests focus on magnetic functional material.

Mr. **Wang Ding** now is a graduate student in the College of Material Science and Technology, NUAA. His research interests focus on magnetic functional material.

Mr. **Huang Guoqiang** is a doctoral candidate in the College of Material Science and Technology, NUAA. His research interests focus on friction stir welding/processing.